Smart polymer surfaces: mapping chemical landscapes on the nanometre scale, Soft Matter, 2010,6, 3764–3768, DOI: 10.1039/C0SM00098A

ARTICLE *in* SOFT MATTER · JUNE 2010

Impact Factor: 4.03 · DOI: 10.1039/C0SM00098A

Smart polymer surfaces: mapping chemical landscapes on the nanometre scale

M. Filimon,[a] I. Kopf,[a] F. Ballout,[a] D. A. Schmidt,[a] E. Bründermann,[a] J. Rühe,[b] S. Santer[c] and M. Havenith*[a]

Received 12th March 2010, Accepted 21st May 2010
DOI: 10.1039/c0sm00098a

We show that Scattering Infrared Near-field Microscopy (SNIM) allows chemical mapping of polymer monolayers that can serve as designed nanostructured surfaces with specific surface chemistry properties on a nm scale. Using s-SNIM a minimum volume of 100 nm × 100 nm × 15 nm is sufficient for a recording of a "chemical" IR signature which corresponds to an enhancement of at least four orders of magnitudes compared to conventional FT-IR microscopy. We could prove that even in cases where it is essentially difficult to distinguish between distinct polymer compositions based solely on topography, nanophase separated polymers can be clearly distinguished according to their characteristic near-field IR response.

Tailoring materials with dynamic switchable responses to external fields is a major goal of modern materials science. Self-assembled monolayers (SAMs) have been used extensively as an extremely flexible route to modify and tailor the surface chemistry of a wide range of metals and metal oxides. SAMs are organic assemblies formed by chemisorption of molecular constituents consisting of an anchor group, a linker chain (which can induce van der Waals interactions with neighboring molecules), and a terminal group which determines the surface properties and the surface chemistry of the material.[1] Due to the self-assembling nature of their formation, it is challenging to obtain large-area defect-free monolayers. Additionally, since they are only several nm thick, they are mechanically and chemically fragile. In the light of these limitations, polymer monolayers are an attractive alternative to build designed nanostructured surfaces that are tailored for specific surface chemistry properties. Polymer brushes are a special case of surface attached layers, where assemblies of macromolecules are chemically bound at one end to the surface with a high grafting density.[2]

Mixed polymer brushes represent systems which consist of two (or more) types of polymer chains where the anchor groups of the different chains are distributed uniformly on the surface. In contrast to conventional brushes, which consist of a single homopolymer, mixed polymer brushes can amplify the response to external stimuli by combining conformational changes and nanophase separation.[3] For example, exposing mixed hydrophilic and hydrophobic brushes to a hydrophilic (hydrophobic) solvent induces a reversible and preferential segregation of the hydrophilic (hydrophobic) component to the surface of the thin film, thus becoming hydrophilic (hydrophobic). Surfaces whose properties dramatically change due to small changes in the environment are also called stimuli-sensitive or "smart" surfaces.[4–8] Such adaptive behavior is very promising for engineering smart surfaces for devices which rely on responses to physical stimuli, such as in biomedical applications[9] and micro- and nano-devices.[10] However, to improve the design of smart surfaces, it is essential to understand the nanophase separation and surface chemistry after exposure to the appropriate physical stimulus.

Although atomic force microscopy (AFM) provides information on topography and local mechanical behavior, it cannot distinguish differing chemical compositions.[11] Fluorescence spectroscopy is highly sensitive, however, it requires chromophore labeling of a specific component[12] and cannot be used for characterization because the chromophore will ultimately change the structure and properties of smart surfaces. Secondary ion mass spectroscopy can provide information of organic surfaces at the nanometre scale, however, the interpretation of spectra is difficult and it is an experimentally complex technique.[13] Scattering scanning near-field infrared microscopy (s-SNIM) is a relatively new technique combining AFM with infrared laser spectroscopy, simultaneously providing both topographic and IR chemical information.[32] It is well-suited for soft matter as it requires no chemical modification, is label free, noninvasive, is not diffraction limited, and probes vibrational modes in the chemical fingerprint region. Knoll and Keilmann showed that s-SNIM is an efficient analytical method that provides spectroscopic characterization of surfaces with nanoscale resolution.[14,15] Indeed, we have previously demonstrated sub-diffraction limited resolution s-SNIM of 90 nm (λ/60) with organic and biological samples.[16] Various heterogeneous systems have been characterized by s-SNIM such as: ion-implanted semiconductor surfaces,[17,18] polymers blends,[14,15,19–21,25] SAMs,[16] lipids,[22] single virus[23] and carbon-like nanoparticles,[24] all with a resolution well below the diffraction limit.

In this study, we demonstrate that SNIM offers the best route to create nanometre-resolved chemical landscape maps of "smart" surfaces without dyes or sample modifications. Here, we present the nanoscale chemical surface analysis of thin-film mixed polymer brushes consisting of poly(styrene-methyl methacrylate) (PS-PMMA) after exposure to different selective solvents.

A commercial dynamic-mode atomic force microscope (AFM) (Nanotec Electronics) was modified to meet our specific

[a]*Lehrstuhl für Physikalische Chemie II, Ruhr-Universität Bochum, Universitätsstr. 150, 44780 Bochum, Germany. E-mail: martina.havenith@rub.de*
[b]*Department of Microsystems Engineering, University of Freiburg—IMTEK, Georges-Koehler-Allee 103, 79110 Freiburg, Germany*
[c]*Institut für Physik und Astronomie, Universität Potsdam, Karl-Leibknecht-Str. 24/25, 14476 Potsdam, Germany*

application. We use commercial gold-coated cantilevers (MikroMasch NSC16/Cr–Au) with a tip curvature radius of 40 nm and resonance frequency of *ca.* 170 kHz. The cantilever is illuminated by a p-polarized beam from a home built liquid nitrogen cooled sealed-off CO laser[26,27] for which the few 100 mW laser power was reduced to mW illuminating power to exclude thermal effects. The laser has more than *ca.* 100 lines with a typical spacing of *ca.* 3 cm^{-1} between subsequent laser lines within the carboxyl absorption band, providing good spectral coverage for our polymer brush films. The near-field scattered light from the tip is collected by a CaF_2 lens and focused onto a liquid nitrogen cooled mercury cadmium telluride detector (MCT, Judson Technologies). We measure the amplitude-modulated near-field signal using phase sensitive lock-in detection on the first harmonic (*i.e.* 340 kHz) to more effectively suppress background signal and increase the signal-to-noise ratio. Fourier transform infrared (FT-IR) spectra were recorded using a Vertex 80v (Bruker) FTIR spectrometer in transmission mode. Each spectrum was averaged over 256 scans with a frequency resolution of 4 cm^{-1} at room temperature. Further details on our experimental set-up can be found in previous publications.[16,17,22] Mixed brushes were prepared by surface-initiated polymerization (grafting from),[28] where two successive grafting steps generate the first polymer, followed by grafting of the second. The brushes consist of two homopolymers, polymethyl methacrylate (PMMA) and polystyrene (PS), covalently bound with one end to a solid substrate. PMMA and PS are immiscible with each other resulting in films showing distinctive nanophase separation in order to avoid unfavorable interactions between polymers.[29] The synthesis of the PS-PMMA mixed brushes investigated here is described in more detail in ref. 5*a*, 5*b*, 30 and 31.

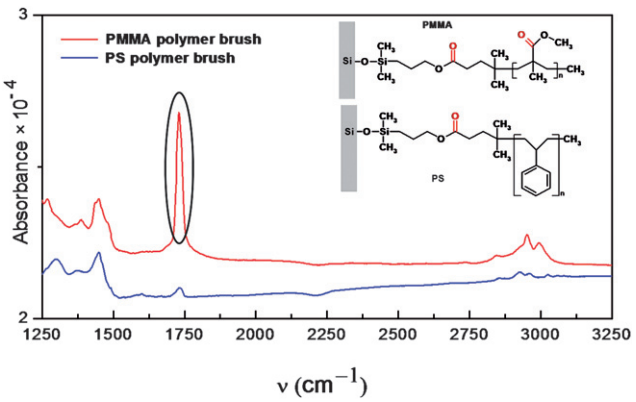

Fig. 1 FTIR absorption spectra of thin-film PS/PMMA homopolymer brushes: PS (blue line) and PMMA (red line). Inset shows chemical structure of both polymers with the carboxyl group for s-SNIM measurements highlighted in red.

Fig. 1 shows FTIR transmission spectra of thin-film (*ca.* 15 nm) PS-PMMA homopolymer brushes. Both brushes show characteristic IR absorption spectra with the most pronounced differences occurring in the C=O and C–H stretching regions. The inset of Fig. 1 shows the chemical structure of the polymer brushes with the C=O group highlighted in red. To maximize the chemical specificity for s-SNIM measurements, the CO laser was tuned across the carboxyl absorption band at *ca.* 1750 cm^{-1}. In addition to FTIR measurements, macroscopic surface properties of the polymer brush films were characterized by contact-angle measurements after exposure to selective solvents.

Fig. 2 shows the topography (left column) for mixed PS/PMMA brushes upon exposure to different solvents. After exposure to acetone, we observe characteristic nanophase

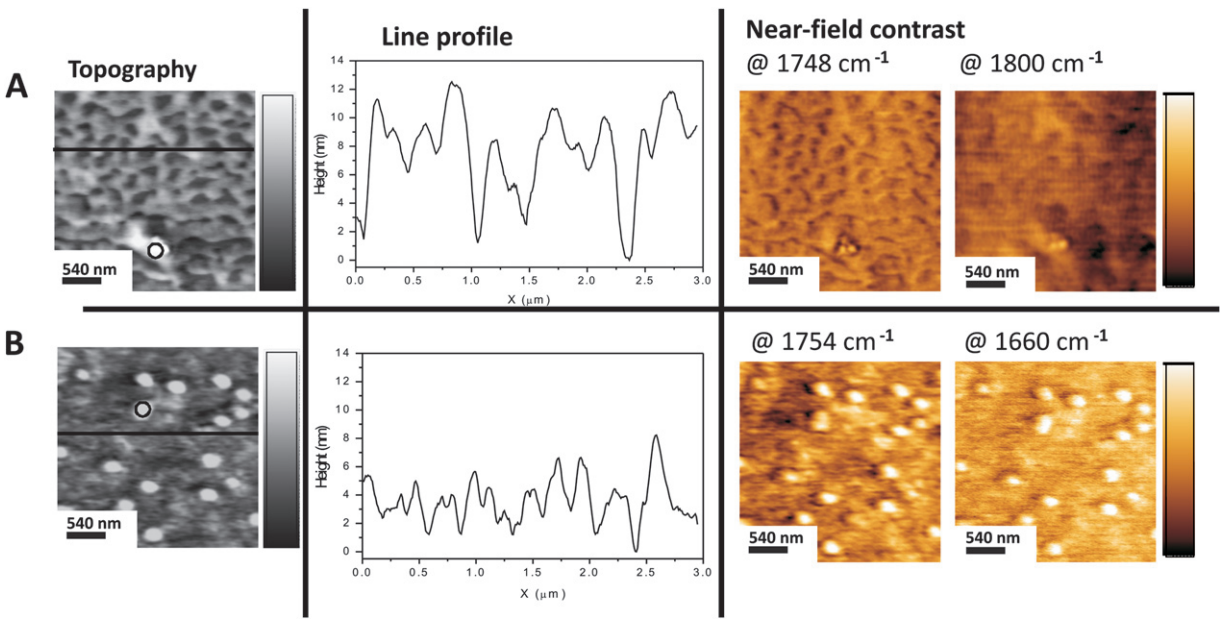

Fig. 2 Simultaneously recorded topographic and near-field images (different wavelenghts) of PS-PMMA polymer brushes after exposure to different solvents: (A) acetone and (B) chloroform. Line scans are along the directions indication in the topographic images. The bright, circular features correspond to 50 nm diameter Si nanoparticles, which are used as a reference (circled areas). Scale bar is 540 nm and scan size is 3 × 3 μm^2.

separation that can easily be seen in the topography (see Fig. 2 line scans). However, after exposure to chloroform, which is a good solvent for both polymers, any topographical evidence for the phase separation is removed[31] showing a very flat topography with a roughness of less than 0.5 nm. Using AFM as the only analytical technique it is therefore not possible to determine unambiguously the surface chemical composition. s-SNIM provides simultaneous information on topography and chemical composition, and is therefore an ideal tool for mapping the chemical landscape of very flat surfaces.

Fig. 2 shows typical s-SNIM images of acetone (A) and chloroform (B) exposed mixed polymer brush films on resonance (1748 cm^{-1} and 1754 cm^{-1}) and off-resonance (1800 cm^{-1} and 1660 cm^{-1}). Chemical specificity is obtained by tuning the CO laser through the C=O absorption band, *e.g.* from *ca.* 1680 cm^{-1} to *ca.* 1800 cm^{-1}, and calculating the wavelength dependence of the contrast. Contrast values, C, are calculated for each wavelength according to:

$$C = 1 - \frac{I_{\text{sample}}}{I_{\text{reference}}} \quad (1)$$

where I_{sample} and $I_{\text{reference}}$ are the scattering intensities of PS (or PMMA) and Si nanoparticles (highlighted by circles in Fig. 2), respectively. Si nanoparticles were used as a reference due to their wavelength-independent response in the IR spectrum.

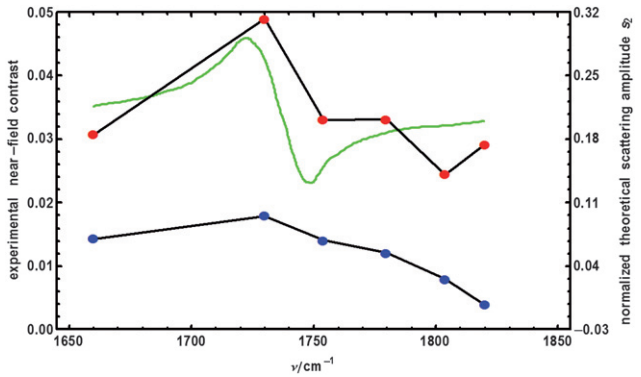

Fig. 3 Experimentally determined average near-field infrared contrast C of the mixed brushes for both PS (blue dots) and PMMA (red dots) (in blue and red). Black lines serve as a guide to the eye. Also shown is the theoretically predicted near-field contrast of PMMA compared to bulk SiO_2 from ref. 33 (green curve).

PMMA shows a characteristic resonance in both the absorption coefficient as well as the refractive index, both of which will contribute to the near-field contrast. As a consequence, the frequency dependence of the contrast C is a convolution of absorption and the refractive index. Fig. 3 shows the frequency dependent near-field contrast of chloroform-exposed PS-PMMA brushes. PS (blue dots) has a weak frequency dependence whereas PMMA (red dots) has a strong frequency dependence, showing a resonance around 1740 cm^{-1} which is attributed to the C=O stretching vibration. For comparison, the theoretically predicted 3rd order scattering amplitude for a 10 nm thick uniform thin-film of PMMA, based on interacting dipoles of a layered system from ref. 33, is shown (green curve). We find very good agreement between the experimentally determined frequency-dependent contrast for PMMA and the theoretical scattering amplitude. We note that comparison of absolute values are difficult due to dependence on a variety of factors including the tip-sample distance, tapping amplitude, laser beam quality, and laser alignment, among others. Nonetheless, the measured frequency dependent contrast shows an unambiguous profile for each compound with a clear resonance at 1740 cm^{-1} for PMMA.

Based on the near-field contrast at 1740 cm^{-1}, we are able to obtain a chemical map of the solvent exposed nanophase separated brushes (Fig. 4, top image). The resulting color-coded chemical image shows the overall distribution of PS-rich (blue)

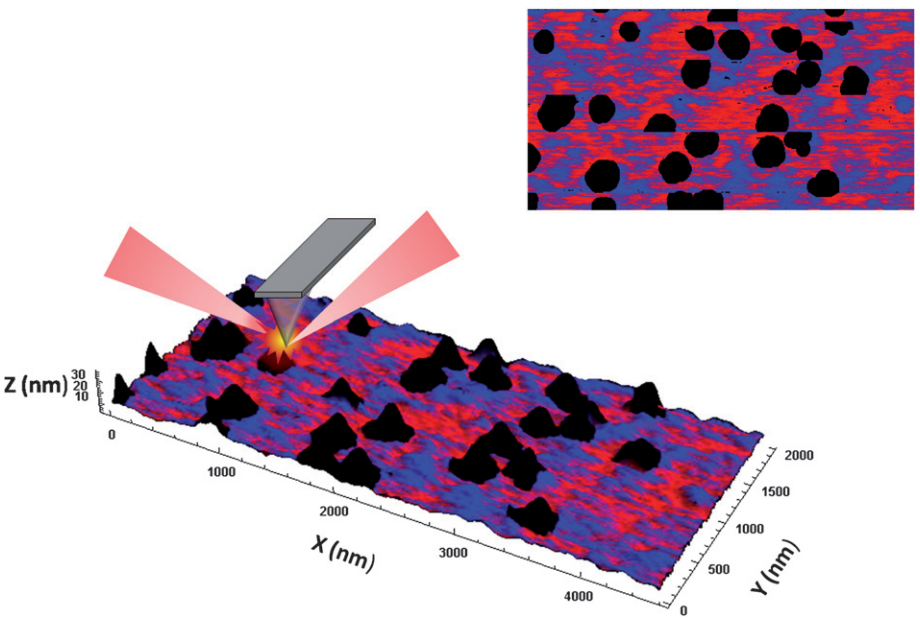

Fig. 4 2D (top) and 3D (bottom) images of 15 nm thick PS-PMMA mixed polymer brushes after exposure to chloroform showing the PMMA-rich (red) and the PS-rich regions (blue). The black objects are the Si nanoparticles used as a reference.

and PMMA-rich (red) regions after exposure to chloroform (see Fig. 4). The black areas mark the Si nanoparticles used for normalizing the near-field contrast combining the simultaneously recorded chemical nanoscopy and topographic information, we can create 3D images of the chemical landscape of mixed polymer brushes. Due to the image segmentation and analysis procedure used to combine AFM and near-field information, "seams" can appear where the data have been segmented, the details of which are beyond the scope of this work.

In the studied sample, the ratio between the total number of PS segments to total number of PMMA segment was calculated to be 1 (50 : 50) and the distance between two neighboring chains is estimated as 4.08 nm.[5] In our reconstructed chemical image (Fig. 4), the ratio between red (PMMA) and blue (PS) areas is displayed. Fig. 4 (2D and 3D images) shows for both polymers a color gradient. That means that the red and blue areas are the areas solely attributed to PMMA and PS, respectively. With decreasing height both areas become purple (blue + red), implying that it is difficult to distinguish between both areas. If we taken into account all pixels that show an unambiguous assignment, a ratio of 47 : 53 for red/blue is obtained, in agreement with our initial assumption.

As can be seen in Fig. 4 (lower image), it is essentially impossible to clearly distinguish between PS and PMMA rich regions based solely on topography, as the blue and red areas show no remarkable height differences. However, both polymers can be clearly distinguished according to their distinct near-field IR contrast (see Fig. 3). The combination of both chemical specificity (s-SNIM) and topography (AFM) can provide critical information on the chemical landscape of polymer surfaces and promises to be a valuable tool for characterizing and improving the design of smart materials on the nanometre scale. Previous measurements proved that the probed area in our set-up corresponds to 90 nm × 90 nm.[16] In the present measurement we determined at the PS/PMMA boundary an increase in contrast (10% to 90%) within 100 nm in agreement with our previous results.

In summary, we have shown that by using s-SNIM we can achieve remarkably high spatial resolution with chemical sensitivity for very thin and flat films. A minimum volume of 100 nm × 100 nm × 15 nm is sufficient for a recording of a "chemical" IR signature using s-SNIM. This increase in sensitivity, by at least four orders of magnitude compared to conventional FTIR microscopy, can be explained by enhancement of the electric fields due to dipole–dipole coupling of the tip with the substrate in close proximity to the surface. This allowed us to obtain characteristic spectral absorption features of polymer brushes on the nanometre scale with no additional sample preparation or modification. s-SNIM should therefore serve as a new and ideal tool in the spectroscopic characterization of polymers, tissues and biomaterials with nanometre resolution.

Acknowledgements

M. Filimon acknowledges financial support by Marie Curie Early Stage Research Training, in the framework of the project INTCHEM (MEST-CT-2005-020681). We acknowledge financial support under grant BMBF 05KS7PC2 for innovative instrumentation of the synchrotron ANKA and by the Deutsche Forschungsgemeinschaft (HA2394/12-1).

References

1 A. Ulman, *Chem. Rev.*, 1996, **96**(4), 1533.
2 (*a*) P. G. de Gennes, *Adv. Colloid Interface Sci.*, 1987, **27**, 189; (*b*) S. J. Alexander, *J. Phys. (Paris)*, 1977, **38**, 983; (*c*) S. T. Milner, *Europhys. Lett.*, 1988, **7**, 695; (*d*) E. B. Zhulina, O. V. Borisov, V. A. Pryamitsyn and T. M. Birshtein, *Macromolecules*, 1994, **24**, 140; (*e*) H. Dong, J. F. Marko and T. A. Witten, *Macromolecules*, 1994, **27**, 6428; (*f*) S. T. Milner, T. A. Witten and M. E. Cates, *Macromolecules*, 1989, **22**, 853.
3 (*a*) K. Matyjaszewski, T. E. Patten and J. H. Xia, *J. Am. Chem. Soc.*, 1997, **119**, 674; (*b*) B. Zhao and W. J. Brittain, *J. Am. Chem. Soc.*, 1999, **121**, 3557; (*c*) B. Zhao, R. T. Haasch and S. MacLaren, *J. Am. Chem. Soc.*, 2004, **126**, 6124; (*d*) M. Müller, *Phys. Rev. E: Stat. Phys., Plasmas, Fluids, Relat. Interdiscip. Top.*, 2002, **65**, 030802(R); (*e*) S. Minko, M. Mueller, D. Usov, A. Scholl, C. Froeck and M. Stamm, *Phys. Rev. Lett.*, 2002, **88**, 035502; (*f*) E. B. Zhulina, C. Singh and A. C. Balazs, *Macromolecules*, 1996, **29**, 6338; (*g*) S. Minko, M. Müller, M. Motornov, M. Nitschke, K. Grundke and M. Stamm, *J. Am. Chem. Soc.*, 2003, **13**, 3896; (*h*) *Polymer Brushes*, ed. R. C. Advincula, W. K. Brittain, K. C. Caster and J. Rühe, Wiley-VCH, Weinheim, Germany, 2004.
4 D. Usov, V. Gruzdev, M. Nitschke, M. Stamm, O. Hoy, I. Luzinov, I. Tokarev and S. Minko, *Macromolecules*, 2008, **40**(24), 8774.
5 (*a*) S. Santer, A. Kopyshev, H.-K. Yang and J. Rühe, *Macromolecules*, 2006, **39**(8), 3056; (*b*) S. A. Santer and J. Rühe, *Polymer*, 2004, **45**, 8279; (*c*) S. G. Boyes, A. M. Granville, M. Baum, B. Akgun and W. J. Brittain, *Surf. Sci.*, 2004, **570**, 1; (*d*) S. Santer, A. Kopyshev, J. Donges, H.-K. Yang and J. Rühe, *Langmuir*, 2006, **22**, 4660.
6 B. Zhao and W. J. Brittain, *Prog. Polym. Sci.*, 2000, **25**, 677.
7 M. Motornov, R. Sheparovych, R. Lupitskyy, E. MacWilliams, O. Hoy, I. Luzinov and S. Minko, *Adv. Funct. Mater.*, 2007, **17**(14), 2307.
8 L. Ionov, M. Stamm and S. Diez, *Nano Lett.*, 2006, **6**(9), 1982.
9 B. Jeong, Y. H. Bae and S. W. Kim, *Nature*, 1997, **388**, 860.
10 L. Ionov and S. Diez, *J. Am. Chem. Soc.*, 2009, **131**(37), 13315.
11 B. Zhao, W. J. Brittain, W. Zhou and S. Z. D. Cheng, *Macromolecules*, 2000, **33**, 8821.
12 D. A. Vanden Bout, W.-T. Yip, D. Hu, D.-K. Fu, T. M. Swager and P. F. Barbara, *Science*, 1997, **277**(5329), 1074.
13 Y.-C. Ning, *Structural Identification of Organic Compounds with Spectroscopic Techniques*, Wiley-VCH, Weinheim, Germany, 2005.
14 B. Knoll and F. Keilmann, *Nature*, 1999, **399**, 134.
15 B. Knoll and F. Keilmann, *Appl. Phys. Lett.*, 2000, **77**(24), 3980.
16 I. Kopf, J.-S. Samson, G. Wollny, Ch. Grunwald, E. Bründermann and H. Havenith, *J. Phys. Chem. C*, 2007, **111**, 8166.
17 J.-S. Samson, G. Wollny, E. Bründermann, A. Bergner, A. Hecker, G. Schwaab, A. D. Wieck and M. Havenith, *Phys. Chem. Chem. Phys.*, 2006, **8**(6), 753.
18 A. Lahrech, R. Bachelot, P. Gleyzes and A. C. Boccara, *Appl. Phys. Lett.*, 1997, **71**, 575.
19 B. Dragnea, J. Preusser, J. M. Szarko, L. A. McDonough, S. R. Leone and W. D. Hinsberg, *Appl. Surf. Sci.*, 2001, **175–176**, 783.
20 T. Taubner, R. Hillenbrand and F. Keilmann, *Appl. Phys. Lett.*, 2004, **85**(21), 5064.
21 K. Mueller, X. Yang, M. Paulite, Z. Fakhraai, N. Gunari and G. C. Walker, *Langmuir*, 2008, **24**, 6946.
22 G. Wollny, E. Bründermann, Z. Arsov, L. Quaroni and M. Havenith, *Opt. Express*, 2008, **16**(10), 7453.
23 M. Brehm, T. Taubner, R. Hillenbrand and F. Keilamm, *Nano Lett.*, 2006, **6**(7), 1307.
24 J.-S. Samson, R. Meißner, E. Bründermann, M. Böke, J. Winter and M. Havenith, *Appl. Phys.*, 2009, **105**(6), 064908.
25 M. B. Raschke, L. Molina, T. Elsaesser, D. H. Kim, W. Knoll and K. Hinrichs, *ChemPhysChem*, 2005, **6**, 2197.
26 U. Merker, P. Engels, F. Madeja, M. Havenith and W. Urban, *Rev. Sci. Instrum.*, 1999, **70**(4), 1933.
27 W. Urban, *Infrared Phys. Technol.*, 1995, **36**(1), 465.
28 (*a*) O. Prucker and J. Rühe, *Langmuir*, 1998, **14**(24), 6893; (*b*) O. Prucker and J. Rühe, *Macromolecules*, 1998, **31**, 592;

(*c*) O. Prucker and J. Rühe, *Macromolecules*, 1998, **31**, 602.
29 S. Santer, A. Kopyshev, J. Donges, H.-K. Yang and J. Rühe, *Adv. Mater.*, 2006, **18**, 2359.
30 A. Kopyshev, Motion of nano-particles by/on polymer brushes, PhD thesis, Albert-Ludwigs Universität Freiburg, 2006.
31 S. Santer, A. Kopyshev, J. Donges, J. Rühe, X. Jiang, B. Zhao and M. Müller, *Langmuir*, 2007, **23**, 279.
32 E. Bründermann and M. Havenith, *Annu. Rep. Prog. Chem., Sect. C*, 2008, **104**, 235.
33 J. Aizpurua, T. Taubner, F. J. García de Abajo, M. Brehm and R. Hillenbrand, *Opt. Express*, 2008, **16**(3), 1529.

